Corrections

MEDICAL SCIENCES

Correction for "Connexin-43 prevents hematopoietic stem cell senescence through transfer of reactive oxygen species to bone marrow stromal cells," by Eri Taniguchi Ishikawa, Daniel Gonzalez-Nieto, Gabriel Ghiaur, Susan K. Dunn, Ashley M. Ficker, Bhuvana Murali, Malav Madhu, David E. Gutstein, Glenn I. Fishman, Luis C. Barrio, and Jose A. Cancelas, which appeared in issue 23, June 5, 2012, of *Proc Natl Acad Sci USA* (109:9071–9076; first published May 18, 2012; 10.1073/pnas.1120358109).

The authors note that both Fig. 1*M* and its legend appeared incorrectly. The corrected figure and its corresponding legend appear below.

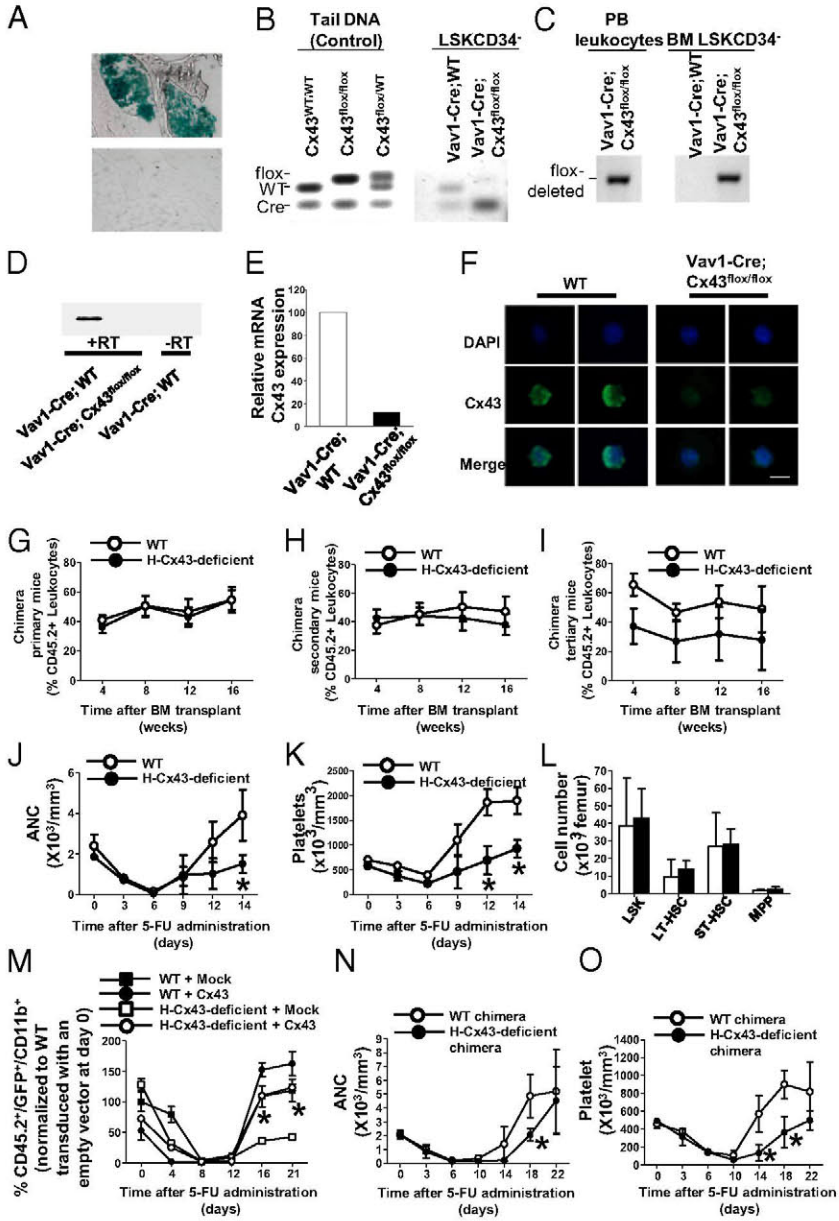

Fig. 1. H-Cx43 deficiency does not impair serial competitive repopulation but impairs the hematopoietic recovery after 5-FU administration. (*A*) Representative example of a longitudinal section of β-galactosidase staining of a femur (original magnification, 40×) from Vav1-Cre; Rosa-loxP-Stop-loxP-LacZ

Legend continued on following page

reporter mice to show presence of recombination in hematopoietic cells. Negative control of BM from non-Cre transgenic littermates is presented (*Lower*). (*B* and *C*) Genomic recombination of Vav1-Cre;Cx43$^{flox/flox}$ LSK CD34$^-$ BM cells (n = pool of 3 mice per group). (*B*) Cx43 floxed vs. WT allele PCR. Cx43 floxed band is practically abrogated in sorted LSK CD34$^-$. Controls of genomic DNA from source animals are also presented for reference. (*C*) Cx43 floxed-out PCR. (*D* and *E*) mRNA expression of Cx43 in HSC/P cells isolated from control and H-Cx43-deficient mice (n = pool of 3 mice per group). (*D*) Semiquantitative RT-PCR for Cx43 expression in LSK CD34$^-$ BM cells. (*E*) Quantitative RT-PCR (Q-RT-PCR) for Cx43 expression in BM MPP. (*F*) Immunofluorescence pictures showing Cx43 (green) along with DAPI (blue) in WT or H-Cx43-deficient HSCs. Cx43 is detected around the cell membrane with asymmetric distribution in most of WT HSCs (n = 20 HSCs from each individual mouse, n = 3 mice per group). (Scale bar, 5 μm.) (*G–I*) Serial competitive repopulation assays. Lethally irradiated primary recipient CD45.1$^+$ mice were transplanted with a mixture of Vav1-Cre; H-Cx43-deficient BM cells (CD45.2$^+$) and WT BM (CD45.1$^+$) cells (solid circle). Control group was transplanted with a mixture of Vav1-Cre; WT BM cells (CD45.2$^+$) and WT BM (CD45.1$^+$) cells (open circle). (*G*) PB chimera analysis was performed at 1, 2, 3, and 4 mo after transplant in primary recipients. (*H*) PB chimera of secondary recipients transplanted with 10×10^6 BM cells obtained from primary mice. (*I*) PB chimera of tertiary recipients transplanted with 10×10^6 BM cells obtained from secondary mice. For competitive repopulation assay, 8–16 mice per group were transplanted and analyzed from 2 independent experiments. (*J* and *K*) PB counts of WT (open circle) or H-Cx43-deficient mice (solid circles) after 5-FU administration. Counts were performed at the indicated days after 5-FU administration. (*J*) Absolute neutrophil counts (ANC). (*K*) Platelet counts. *$P <$ 0.05 (n = 3 mice per group in each of two independent experiments). (*L*) HSC and MPP content of BM on day 21 after 5-FU treatment. (*M*) Transplant of HSC/P cells transduced with a Cx43-expressing lentiviral vector rescues PB recovery after 5-FU administration in H-Cx43-deficient mice. Recipient mice were transplanted with LSK BM cells transduced with an empty vector or a Cx43-expressing lentiviral vector. After 4 wk posttransplantation, recipient mice were administered 5-FU and PB cell counts and flow cytometric analysis of myeloid (CD11b) recovery were performed at the indicated days after 5-FU administrations. ■, WT with empty vector transduction (WT + Mock); ●, WT with Cx43 transduction (WT + Cx43): □, H-Cx43-deficient with empty vector transduction (H-Cx43-deficient + Mock); ○, H-Cx43-deficient with Cx43 transduction (H-Cx43-deficient + Cx43). *$P < 0.05$ (n = 4 mice/group in each of two independent experiments). Values represent means ± SD. (*N* and *O*) Lethally irradiated primary recipient CD45.1$^+$ mice were transplanted with H-Cx43-deficient BM cells (CD45.2$^+$) or Vav1-Cre; WT BM cells (CD45.2$^+$). PB count of WT (open circle) or H-Cx43-deficient mice (solid circle) after 5-FU administration were analyzed after 4 wk post transplant. (*N*) Absolute neutrophil count (ANC). (*O*) Platelet count. *$P < 0.05$ (n = 5 mice per group). Values represent means ± SD.

PSYCHOLOGICAL AND COGNITIVE SCIENCES

Correction for "Exposure therapy triggers lasting reorganization of neural fear processing," by Katherina K. Hauner, Susan Mineka, Joel L. Voss, and Ken A. Paller, which appeared in issue 23, June 5, 2012, of *Proc Natl Acad Sci USA* (109:9203-9208; first published May 23, 2012; 10.1073/pnas.1205242109).

The authors note that the x/y/z coordinates listed for brain regions in Table 1 appeared incorrectly. The corrected table appears below. This error does not affect the conclusions of the article.

Table 1. Summary of fMRI activity clusters

						Baseline, phobogenic vs. neutral		Baseline vs. posttherapy		Posttherapy vs. follow-up	
Region (BA)	L/R/B	Volume (mm^3)	*x*	*y*	*z*	*t*	*P*	*t*	*P*	*t*	*P*
Fig 1. regions shown in blue											
Posterior cingulate (BA 31)	B	8,343	4	−40	49	1.77	0.10	−2.82	0.02	2.03	0.07
Anterior cingulate/ vmPFC (BA 24, 32)	B	7,965	−3	20	27	3.19	0.01	−3.11	0.01	NS	
Anterior insula (BA 13)	L	2,187	−53	8	−1	2.09	0.06	−2.70	0.02	NS	
Anterior insula (BA 13)	R	1,782	37	6	6	3.91	0.00	−2.46	0.03	NS	
Posterior insula (BA 13, 19)	R	8,478	47	−45	13	2.33	0.04	−2.81	0.02	NS	
Middle temporal gyrus (BA 39)	L	1,134	−41	−51	7	3.77	0.00	−2.71	0.02	NS	
Medial frontal gyrus (BA 6)	R	1,809	6	−15	67	2.68	0.02	−2.48	0.03	NS	
Amygdala (anatomically defined)	R	891	n/a	n/a	n/a	3.65	0.00	−4.59	0.00	NS	
Fig 1. region shown in red											
dlPFC (BA 6, 8)	R	918	36	15	61	−2.38	0.04	8.27	0.00	−2.63	0.02
Superior parietal lobule (BA 7)	R	1,458	25	−72	57	NS		3.12	0.01	NS	
Fig. 2 regions shown in gray											
Fusiform/lingual gyrus (BA 18, 19)	L	8,046	−34	−81	−9	4.91	0.00	NS		−5.10	0.00
Fusiform/lingual gyrus (BA 18, 19)	R	11,367	36	−78	−11	5.14	0.00	NS		−5.36	0.00

For each activity cluster, listed are Brodmann areas (BA), hemisphere [left (L), right (R), or bilateral (B)], the volume (mm^3), and stereotactic coordinates for the centrally activated voxel (*x, y, z* mm). Statistics are reported for all *P* values ≤ 0.10, and otherwise listed as nonsignificant (NS).

Connexin-43 prevents hematopoietic stem cell senescence through transfer of reactive oxygen species to bone marrow stromal cells

Eri Taniguchi Ishikawa [a], Daniel Gonzalez-Nieto [a], Gabriel Ghiaur [b], Susan K. Dunn [a], Ashley M. Fickler [a], Bhuvana Murali [a], Malav Madhu [a], David E. Gutstein [c], Glenn I. Fishman [c], Luis C. Barrio [d], and Jose A. Cancelas [a,e]

[a]Research Division, Hoxworth Blood Center, University of Cincinnati, Cincinnati, OH 45267; [b]Stem Cell Program, Division of Experimental Hematology and Cancer Biology, Cincinnati Children's Hospital Medical Center, Cincinnati, OH 45229; [c]Leon H. Charney Division of Cardiology, New York University School of Medicine, New York, NY 10016; [d]Merck Sharp & Dohme Corporation, Rahway, NJ, 07065; and [e]Unit of Experimental Neurology, Department of Research, Hospital Ramon y Cajal, 28034 Madrid, Spain

Hematopoietic stem cell (HSC) aging has become a concern in chemotherapy of older patients. Humoral and paracrine signals from the bone marrow (BM) hematopoietic microenvironment (HM) control HSC activity during regenerative hematopoiesis. Connexin-43 (Cx43), a connexin constituent of gap junctions (GJs) is expressed in HSCs, down-regulated during differentiation, and postulated to be a self-renewal gene. Our studies, however, reveal that hematopoietic-specific Cx43 deficiency does not result in significant long-term competitive repopulation deficiency. Instead, hematopoietic Cx43 (H-Cx43) deficiency delays hematopoietic recovery after myeloablation with 5-fluorouracil (5-FU). 5-FU-treated H-Cx43-deficient HSC and progenitors (HSC/P) cells display decreased survival and fail to enter the cell cycle to proliferate. Cell cycle quiescence is associated with down-regulation of cyclin D1, up-regulation of the cyclin-dependent kinase inhibitors, $p21^{cip1}$ and $p16^{INK4a}$, and Forkhead transcriptional factor 1 (Foxo1), and activation of p38 mitogen-activated protein kinase (MAPK), indicating that H-Cx43-deficient HSCs are prone to senescence. The mechanism of increased senescence in H-Cx43-deficient HSC/P cells depends on their inability to transfer reactive oxygen species (ROS) to the HM, leading to accumulation of ROS within HSCs. In vivo antioxidant administration prevents the defective hematopoietic regeneration, as well as exogenous expression of Cx43 in HSC/P cells. Furthermore, ROS transfer from HSC/P cells to BM stromal cells is also rescued by reexpression of Cx43 in HSC/P. Finally, the deficiency of Cx43 in the HM phenocopies the hematopoietic defect in vivo. These results indicate that Cx43 exerts a protective role and regulates the HSC/P ROS content through ROS transfer to the HM, resulting in HSC protection during stress hematopoietic regeneration.

Gja1 | stem cell niche

Blood cell formation in the bone marrow (BM) is dependent on the close association of developing hematopoietic cells with supporting stromal cells. These hematopoietic demands are filled by a pool of hematopoietic stem cells (HSCs) with self-renewal and multipotential differentiation ability. The BM hematopoietic microenvironment (HM) has been shown to have a crucial role that influences the proliferative activity and differentiation process of HSCs and progenitors (HSC/P) by positive and negative humoral and paracrine signals.

Gap junctions (GJs) represent a system of direct cell-to-cell intercellular communication (IC) (1). Although the existence of GJs in BM has been known for over 30 y, their function remains unclear (2, 3). GJ channels are formed by dodecamers of protein subunits called connexins (Cxs). Cx43 is the predominant Cx expressed in the BM, thymus, spleen, and other lymphoid tissues (4–6). Cx43 has been shown to be part of the signature of HSCs (7–9), being down-regulated during differentiation to progenitors (7) and up-regulated in the endosteal space of the BM following cytoablative therapy (6). Its deficiency in the BM results in deficient hematopoietic regeneration after in vivo challenge with 5-fluorouracil (5-FU) (10), which is an established stressor of quiescent HSCs (11). However, a mechanistic analysis of the role of Cx43 in hematopoietic regeneration has not been addressed. In this report, we present compelling data unveiling a mechanism of ROS detoxification in HSCs through Cx43-dependent transfer to the HM that prevents HSC quiescence/senescence after myeloablation.

Results

To clarify whether Cx43 plays a crucial role in HSCs and to elucidate the mechanism of impaired hematopoietic recovery after in vivo 5-FU challenge, we have generated a mouse model with constitutive deficiency of Cx43 in hematopoiesis [Vav1-Cre/$Cx43^{flox/flox}$, hematopoietic specific (H)-Cx43-deficient]. As reported by others (12–15), we confirmed that Vav1-Cre expression is extremely efficient, inducing recombination of either a reporter gene (Fig. 1*A*) or the floxed *Gja1* ($Cx43^{flox/flox}$) gene (Fig. 1 *B* and *C*). The mRNA expression of Cx43 in HSCs from Vav1-Cre;$Cx43^{flox/flox}$ mice was practically abolished in BM HSCs [defined as $lineage^-$/c-kit^+/Sca-1^+/$CD34^-$ (LSK $CD34^-$); Fig. 1*D*] and multipotential progenitors (MPPs) (defined as LSK/$CD34^+$; Fig. 1*E*). Furthermore, we analyzed the protein expression of Cx43 in wild-type (WT) and Vav1-Cre;$Cx43^{flox/flox}$ HSCs. Confocal microscopy detected Cx43 protein expression in the membrane of isolated HSCs from WT but not from Vav1-Cre;$Cx43^{flox/flox}$ mice (Fig. 1*F*). Expression of Cx45 (Gjc1), another connexin family protein involved in hematopoiesis, was detected in both WT and Vav1-Cre;$Cx43^{flox/flox}$ HSCs (Fig. S1) and was found not to be significantly up-regulated in H-Cx43-deficient HSCs (Table S1). Cx37 (Gja8) and Cx50 (Gja4) showed marginal mRNA expression up-regulation trends (Table S1). Thus, the deficiency of Cx43 in HSCs was not associated with significant compensatory up-regulation of other connexins.

To examine whether the loss of Cx43 expression in HSCs impairs the BM HSC content and function, we first analyzed the peripheral blood (PB) counts (Fig. S2*A*) and content of

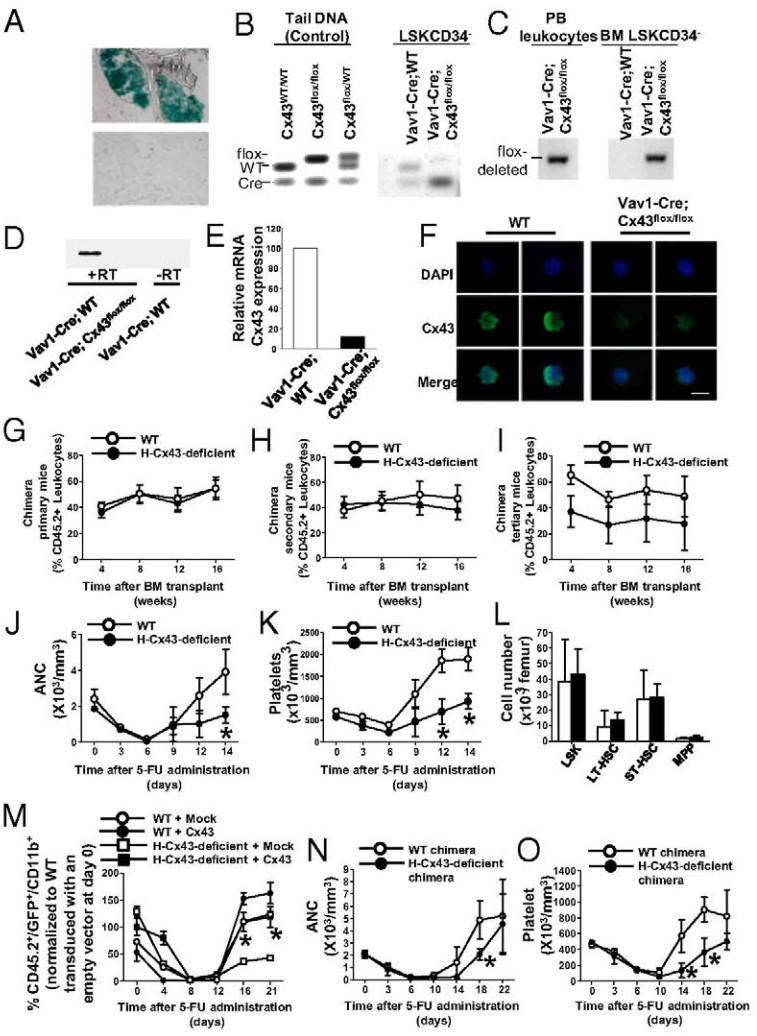

Fig. 1. H-Cx43 deficiency does not impair serial competitive repopulation but impairs the hematopoietic recovery after 5-FU administration. (*A*) Representative example of a longitudinal section of β-galactosidase staining of a femur (original magnification, 40×) from Vav1-Cre; Rosa-loxP-Stop-loxP-LacZ reporter mice to show presence of recombination in hematopoietic cells. Negative control of BM from non-Cre transgenic littermates is presented (*Lower*). (*B* and *C*) Genomic recombination of Vav1-Cre;$Cx43^{flox/flox}$ LSK $CD34^-$ BM cells (n = pool of 3 mice per group). (*B*) Cx43 floxed vs. WT allele PCR. Cx43 floxed band is practically abrogated in sorted LSK $CD34^-$. Controls of genomic DNA from source animals are also presented for reference. (*C*) Cx43 floxed-out PCR. (*D* and *E*) mRNA expression of Cx43 in HSC/P cells isolated from control and H-Cx43-deficient mice (n = pool of 3 mice per group). (*D*) Semiquantitative RT-PCR for Cx43 expression in LSK $CD34^-$ BM cells. (*E*) Quantitative RT-PCR (Q-RT-PCR) for Cx43 expression in BM MPP. (*F*) Immunofluorescence pictures showing Cx43 (green) along with DAPI (blue) in WT or H-Cx43-deficient HSCs. Cx43 is detected around the cell membrane with asymmetric distribution in most of WT HSCs (n = 20 HSCs from each individual mouse, n = 3 mice per group). (Scale bar, 5 μm.) (*G–I*) Serial competitive repopulation assays. Lethally irradiated primary recipient $CD45.1^+$ mice were transplanted with a mixture of Vav1-Cre; H-Cx43-deficient BM cells ($CD45.2^+$) and WT BM ($CD45.1^+$) cells (solid circle). Control group was transplanted with a mixture of Vav1-Cre; WT BM cells ($CD45.2^+$) and WT BM ($CD45.1^+$) cells (open circle). (*G*) PB chimera analysis was performed at 1, 2, 3, and 4 mo after transplant in primary recipients. (*H*) PB chimera of secondary recipients transplanted with 10×10^6 BM cells obtained from primary mice. (*I*) PB chimera of tertiary recipients transplanted with 10×10^6 BM cells obtained from secondary mice. For competitive repopulation assay, 8–16 mice per group were transplanted and analyzed from 2 independent experiments. (*J* and *K*) PB counts of WT (open circle) or H-Cx43-deficient mice (solid circles) after 5-FU administration. Counts were performed at the indicated days after 5-FU administration. (*J*) Absolute neutrophil counts (ANC). (*K*) Platelet counts. $^*P <$ 0.05 (n = 3 mice per group in each of two independent experiments). (*L*) HSC and MPP content of BM on day 21 after 5-FU treatment. (*M*) Transplant of HSC/P cells transduced with a Cx43-expressing lentiviral vector rescues PB recovery after 5-FU administration in H-Cx43-deficient mice. Recipient mice were transplanted with LSK BM cells transduced with an empty vector or a Cx43-expressing lentiviral vector. After 4 wk posttransplantation, recipient mice were administered 5-FU and PB cell counts and flow cytometric analysis of myeloid (CD11b) recovery were performed at the indicated days after 5-FU administrations. ○, WT with empty vector transduction (WT + Mock); ●, WT with Cx43 transduction (WT + Cx43); □, H-Cx43-deficient with empty vector transduction (H-Cx43-deficient + Mock); ■, H-Cx43-deficient with Cx43 transduction (H-Cx43-deficient + Cx43). $^*P < 0.05$ (n = 4 mice/group in each of two independent experiments). Values represent means ± SD. (*N* and *O*) Lethally irradiated primary recipient $CD45.1^+$ mice were transplanted with H-Cx43-deficient BM cells ($CD45.2^+$) or Vav1-Cre; WT BM cells ($CD45.2^+$). PB count of WT (open circle) or H-Cx43-deficient mice (solid circle) after 5-FU administration were analyzed after 4 wk post transplant. (*N*) Absolute neutrophil count (ANC). (*O*) Platelet count. $^*P < 0.05$ (n = 5 mice per group). Values represent means ± SD.

phenotypically identifiable BM HSC/P populations. We found no significant differences in blood counts or the content of Lin^-/c-kit^+ (LK), LSK, MPP, or HSC populations in H-Cx43-deficient mice (Fig. S2*B*). Second, the HSC content and function were assessed in vivo, using serial competitive repopulation assays. HSCs from H-Cx43-deficient mice exhibited no significant defect in their competitive engraftment and lineage hematopoiesis regeneration (Fig. S3) in the primary (Fig. 1*G*), secondary (Fig. 1*H*), and tertiary recipient mice (Fig. 1*I*).

Hematopoietic stress induced by 5-FU has been used to test the ability of HSCs to recover homeostatic blood formation (16). After a period of pancytopenia, the magnitude of the compensatory BM regeneration phase indicates the functional reserve of HSCs (17). Repeated administration of 5-FU to mice induces exhaustion of the normal HSC pool and a progressive inability to recover (18), indicating HSC damage. Similarly to mice in which both HSCs and the HM are H-Cx43-deficient (10), H-Cx43-deficient mice treated with 5-FU (150 mg/kg i.v.) lack a hyperregenerative response phase, as demonstrated by an abrogated rebound in neutrophil (Fig. 1*J*) and platelet (Fig. 1*K*) counts in PB, indicating a loss of hematopoietic response activity after stress. This deficiency is not persistent because the content of HSCs and MPPs in the BM by day 21 after 5-FU challenge is similar to WT levels (Fig. 1*L*). The myeloid regeneration of H-Cx43-deficient animals after 5-FU administration is completely rescued in hematopoietic chimeric mice, where hematopoietic Cx43 expression has been reintroduced through transplantation of lentivirally transduced LSK cells (Fig. 1*M*). Altogether, there results indicate that hematopoietic Cx43 expression is critical for hematopoietic regeneration after 5-FU administration. Finally, the reduced hematopoietic regeneration of H-Cx43-deficient HSCs was confirmed in full chimeras of WT or H-Cx43-deficient BM (Fig. 1 *N* and *O*), supporting a cell autonomous role of Cx43.

To examine the underlying cellular mechanism responsible for the impaired hematopoietic recovery after 5-FU administration in H-Cx43-deficient mice, we analyzed the proliferation status of H-Cx43-deficient BM $Lin^-/CD41^-/CD48^-/CD150^+$ cells, which also define phenotypically the HSC population (19, 20) and is not affected by down-regulation of c-kit expression during hematopoietic regeneration (21) after 5-FU administration. We

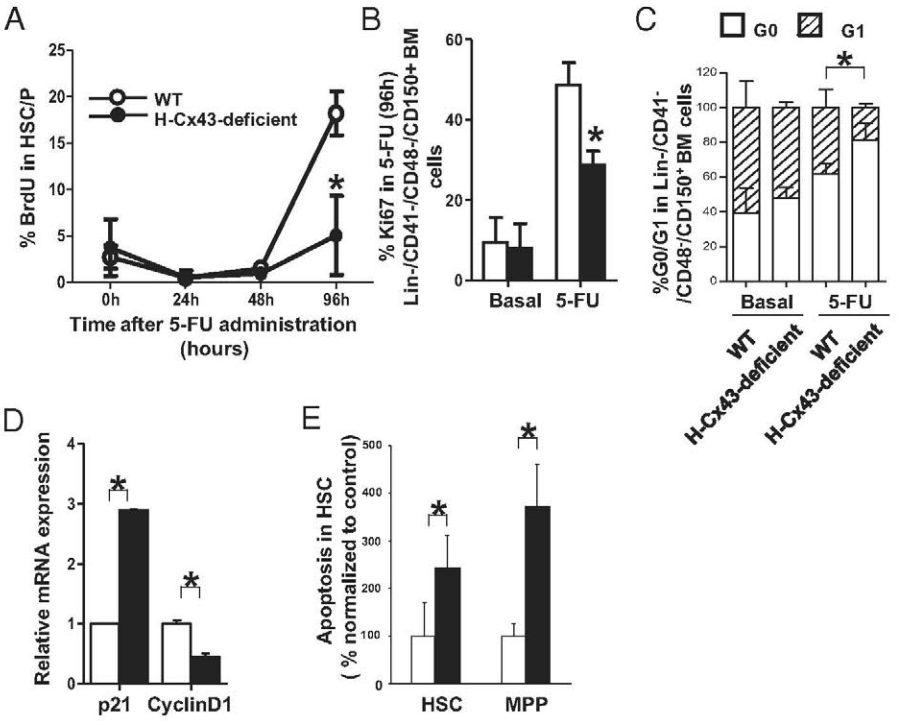

Fig. 2. H-Cx43-deficient HSCs are impaired to enter cell cycle to proliferate and have decreased cell survival after 5-FU administration. (*A*) Kinetics of BrdU incorporation in HSCs after 5-FU administration. Proliferation of BM-Lin$^-$CD41$^-$CD48$^-$CD150$^+$ cells in WT or H-Cx43-deficient mice was measured by analysis of BrdU incorporation at 24, 48, and 96 h after 5-FU administration in vivo. Analysis in WT (open circles) or H-Cx43-deficient (solid circles) mice are presented. *$P < 0.05$ (a minimum of three mice per group in two independent experiments was analyzed). (*B*) Proliferation of BM-Lin$^-$CD41$^-$CD48$^-$CD150$^+$ cells after 5-FU administration in WT or H-Cx43-deficient mice was measured by analysis of Ki67 staining in vivo. Analysis in WT (open bars) or H-Cx43-deficient (solid bars) mice are presented. *$P < 0.05$ ($n = 3$ mice per group in each of two independent experiments). (*C*) Pyronin/7-AAD Y cell cycle analysis of WT or H-Cx43-deficient BM after in vivo 5-FU administration. □, G0 phase; hashed box, G1 phase. *$P < 0.05$ ($n = 3$ mice per group in each of two independent experiments). (*D*) Q-RT-PCR for p21 and cyclinD1 expression in Lin$^-$CD41$^-$CD48$^-$CD150$^+$ BM cells. Analysis in WT (open bars) or H-Cx43-deficient (solid bars) mice are presented. *$P < 0.05$. (*E*) Frequency of apoptotic (active caspase-3-expressing) cells on HSC and MPP cell populations after 5-FU administration in vivo. Data from WT (open bars) or H-Cx43-deficient mice (solid bars) are presented. *$P < 0.05$.

first analyzed the frequency of HSCs in DNA synthesis phase in vivo at 0, 24, 48, and 96 h after 5-FU administration. Whereas WT BM HSCs showed a ~fourfold increase in the frequency of HSCs in S phase between days 2 and 4 after 5-FU administration (Fig. 2*A*), H-Cx43-deficient HSCs did not significantly cycle, as assessed by lack of increase in bromodeoxyuridine (BrdU) uptake (Fig. 2*A*) or expression of Ki67 (Fig. 2*B* and Fig. S4*A*), by 96 h after 5-FU administration compared with WT HSCs, which confirmed an impaired cell cycle entry in response to chemotherapeutic stress. Pyronin/7-aminoactinomycin D (7-AAD) staining showed accumulation of H-Cx43-deficient HSCs in the G_0 phase of the cell cycle (Fig. 2*C* and Fig. S4*B*), indicating that 5-FU treated H-Cx43-deficient HSCs also failed to transit through the G_0/G_1 checkpoint. Pathway analysis of the differential transcriptional expression of 5-FU (96 h)-treated H-Cx43-deficient HSCs suggested significant impairment of the transition through cell cycle checkpoints (Table S2), and Q-RT-PCR confirmed the up-regulation of the cyclin dependent kinase $p21^{cip1}$ and down-regulation of cyclin D1 mRNA levels in 5-FU (96 h)-treated H-Cx43-deficient HSCs (Fig. 2*D*). In addition, HSCs (and MPPs) from H-Cx43-deficient mice showed increased apoptosis in vivo (Fig. 2*E*) and activation of cell death genes (Table S2).

We next determined the molecular mechanisms associated with HSC impaired cell cycle entry in the live gated cell fraction of 5-FU-treated H-Cx43-deficient HSCs. We analyzed the expression and activation through Ser-10 phosphorylation of p53 in H-Cx43-deficient HSCs after 5-FU administration, which is associated with HSC quiescence. We found that H-Cx43-deficient HSCs from unchallenged mice expressed a ~2.5-fold higher level of activated p53. In 5-FU-treated H-Cx43-deficient HSCs, the activation of p53 (Fig. 3*A* and Fig. S5) or its downstream targets Gadd45a, Pimp1, and Bmi1 (Fig. 3*B*) were similar to WT HSCs. In contrast to p53-dependent HSC quiescence, HSC senescence depends on up-regulated expression of the cyclin-dependent kinase inhibitor $p16^{INK4a}$, a hallmark of stem cell aging (22). There was a ~twofold increase in the expression of nuclear $p16^{INK4a}$, which is up-regulated during cell senescence (22), in both unchallenged and in vivo 5-FU-challenged H-Cx43-deficient HSCs (Fig. 3*C*). In addition, there was a ~twofold up-regulation of the expression of Rb1, a central regulator of the G_1 phase of the cell cycle and a regulator of interactions between HSCs and the HM (Table S2) (23). These results indicate that the H-Cx43-deficient HSCs are prone to senescence under stress.

A major pathway of p16 up-regulation in HSC senescence is ROS-dependent activation of p38 (24). Pathway analysis of the top signaling pathways differentially expressed by 5-FU-treated H-Cx43-deficient HSCs showed a statistically significant activation of oxidative damage in 5-FU-treated HSCs from H-Cx43-deficient mice (Table S2). Analysis of the intracellular levels of ROS (H_2O_2 and O_2^-) in WT and H-Cx43-deficient HSCs after 5-FU administration, showed that H-Cx43-deficicient HSCs after 5-FU administration had an ~1.8- to 2.1-fold increase in intracellular ROS content compared with WT HSCs (Fig. 3 *D* and *E*). The production of ROS is one of the byproducts of mitochondrial respiration, and mitochondrias have frequently been considered as the main source of cellular-

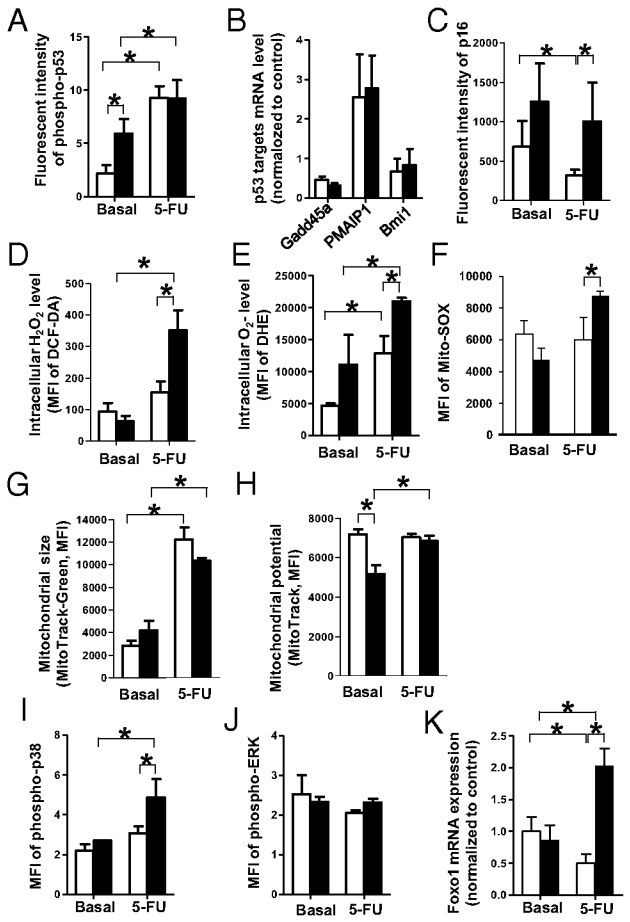

Fig. 3. Cell cycle arrest in H-Cx43-deficient after 5-FU treatment is associated with increased levels of intracellular ROS and activation of quiescence markers p16 and p38. (*A*) Immunofluorescence intensity of anti-phopho-p53 immunostaining of BM-Lin$^-$CD41$^-$CD48$^-$CD150$^+$ cells from WT (open bars) or H-Cx43-deficient mice (solid bars) after 5-FU administration was measured by using computer-imaging software (Axiovision; Zeiss). *$P < 0.05$ ($n = 20$–35 cells per group were measured from a minimum of two mice per group). (*B*) Q-RT-PCR of p53 downstream targets in BM-Lin$^-$CD41$^-$CD48$^-$CD150$^+$ cells, isolated from WT (open bars) and H-Cx43-deficient mice (solid bars) after 5-FU administration. (*C*) Immunofluorescence intensity of anti-p16 immunostaining of BM-Lin$^-$CD41$^-$CD48$^-$CD150$^+$ cells from WT (open bars) or H-Cx43-deficient mice (solid bars) after 5-FU administration. *$P < 0.05$ ($n = 20$–35 cells per group were measured from a minimum of 2 mice per group). (*D–F*) Intracellular H_2O_2 level measured with DCF-DA (*D*), intracellular O_2^- level measured with DHE (*E*) and mitochondrial-derived superoxide levels (*F*) in BM-Lin$^-$CD41$^-$CD48$^-$CD150$^+$ cells from WT (open bars) or H-Cx43-deficient mice (solid bars) after 5-FU administration. *$P < 0.05$ ($n = 3$ mice per group in each of two independent experiments). (*G* and *H*) Mitochondrial size (MitoTracker Green FM) (*G*) and mitochondrial potential (MitoTrackerRed FM) (*H*) of BM-Lin$^-$CD41$^-$CD48$^-$CD150$^+$ cells after 5-FU administration in WT (open bars) or H-Cx43-deficient mice (solid bars) were measured in vivo. *$P < 0.05$ ($n = 3$ mice per group). (*I* and *J*) Mean fluorescent intensity of phospho-p38 (*I*) and phospho-MAPK (*J*) of BM-Lin$^-$CD41$^-$CD48$^-$CD150$^+$ cells from WT (open bars) or H-Cx43-deficient mice (solid bars) after 5-FU administration. *$P < 0.05$ ($n = 3$ mice per group in each of two independent experiments). (*K*) Q-RT-PCR for Foxo1 expression in BM-Lin$^-$CD41$^-$CD48$^-$CD150$^+$ cells, isolated from WT (open bars) and H-Cx43-deficient mice (solid bars) after 5-FU administration *$P < 0.05$ (pool of three mice per group). Values represent means ± SD.

derived ROS (25). Mitochondrial Cx43 has been shown to play a role in mediating the cardioprotective effect of ischemic preconditioning through modification of the mitochondrial content and membrane potential (26). Analysis of O_2^- generated by mitochondrial activity showed that, similarly to overall intracellular ROS levels, mitochondrial-derived superoxide levels were increased in 5-FU-treated H-Cx43-deficient HSCs compared with WT HSCs (Fig. 3*F*). However, the mitochondrial mass was not affected and the mitochondrial membrane potential only marginally decreased in unchallenged H-Cx43-deficient HSCs but not after 5-FU administration (Fig. 3 *G* and *H*), indicating that the deficiency of Cx43 does not correlate with significant modifications in mitochondrial mass or membrane potential. Moreover, increased ROS levels correlated with increased p38 activation (Fig. 3*I*) but not extracellular signal-regulated kinase (Erk) activation (Fig. 3*J*). Activation of p38 correlated with Foxo1 expression (Fig. 3*K*), which, in addition to $p16^{INK4a}$ up-regulation, have been shown to be hallmarks of ROS-dependent HSC repopulation loss-of-function (24) and HSC resistance to physiologic oxidative stress (27), respectively.

Transfer of small molecules is arguably a well-recognized function of Cx43-dependent channels (28). We hypothesized that Cx43 deficiency would lead to accumulated levels of intracellular ROS in HSCs, resulting in cell cycle arrest, apoptosis, and senescence. To test this hypothesis, we performed a set of mechanistic experiments to address the role of Cx43 in the control of HSC ROS content. First, we tested whether antioxidant therapy with *N*-acetyl-L-cysteine (NAC), a reducing agent that diminishes the endogenous level of intracellular ROS, could reverse the impaired hematopoietic regeneration of H-Cx43-deficient mice after 5-FU administration. WT or H-Cx43-deficient animals were treated daily with NAC or control vehicle starting 1 d before 5-FU administration. There was a complete restoration of the neutrophil and platelet count recovery in H-Cx43-deficient mice after in vivo treatment with NAC to the levels seen in WT mice treated with PBS or NAC (ANOVA; $P < 0.05$ for both neutrophil and platelet counts) (Fig. 4 *A* and *B*). These data prove that oxidative stress is causal in the hematopoietic recovery delay of H-Cx43-deficient HSCs after 5-FU administration.

Second, it has been shown that Cx43 mediates BM stromal cell adhesion to HSCs (29). To address whether the contact of HSCs with BM stromal cells was causal in the control of HSC ROS levels, we cocultured HSC/P cells derived from WT or H-Cx43-deficient mice with preplated FBMD-1 stromal cells, a well-recognized model of heterocellular hematopoiesis-supporting stroma (30) composed of ROS^{high} and ROS^{low} cell populations (Fig. S6). We then analyzed whether ROS could be efficiently transferred from WT HSC/P cells to BM stromal cells. Before culture, primary sorted HSC/P cells were treated with LY83583 (6-anilino-5,8-quinolinequinone), a generator of superoxide anions (31), to model increased ROS production as seen in vivo after 5-FU administration; and BM stromal cells were treated with NAC, to diminish basal ROS levels. The intracellular concentration of ROS in HSC/P cells was measured in sorted HSC/P cells by flow cytometric analysis of fluorescence intensity of dihydroethidium (DHE), an O_2^- reporter that binds to DNA irreversibly upon oxidation becoming unavailable to be transferred through GJs. When HSC/P cells were plated without FBMD-1 stroma as a control, LY83583-treated WT or H-Cx43-deficient HSC/P cells showed high intracellular ROS levels (Fig. 4*C*). When WT HSC/P cells were cultured onto FBMD-1 cells, however, the intracellular ROS levels in WT HSC/P cells diminished significantly (~83% reduction; $P < 0.001$) compared with H-Cx43-deficient HSC/P cells (Fig. 4*C*). Although FBMD-1 cells maintained their ability to reduce ROS content of H-Cx43-deficient HSC/P cells (~64% reduction; $P = 0.02$), they did so to a lesser degree ($P = 0.03$) than in WT HSC/P, indicating that the ability of FBMD-1 cells to diminish ROS concentration in HSC/P cells is lessened by the Cx43 deficiency in HSC/P cells.

Third, if ROS transfer is the mechanism of ROS scavenging, then culture of high ROS-containing HSC/P cells onto FBMD-1 cells should increase the intracellular levels of ROS in the

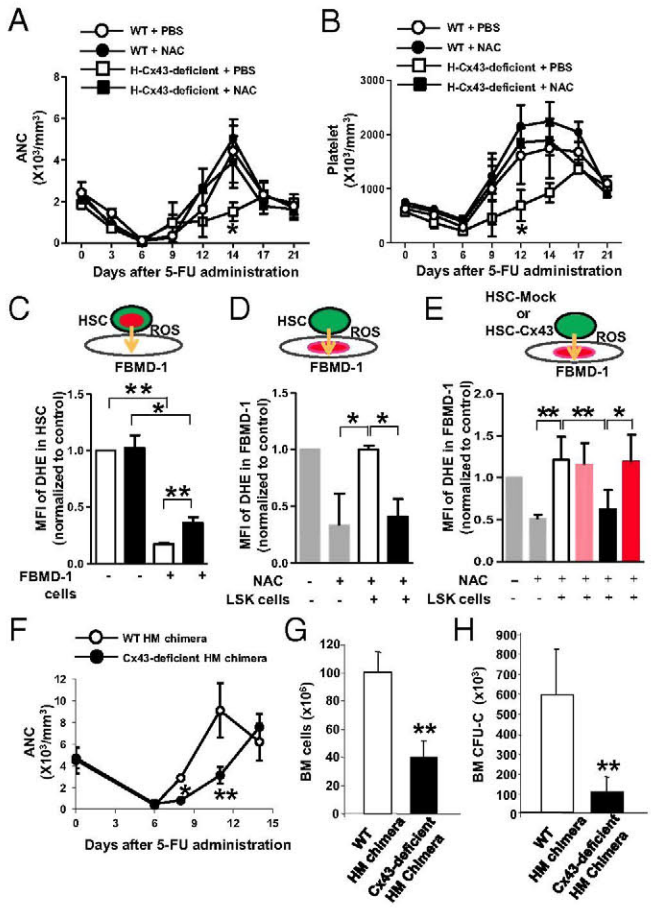

Fig. 4. Antioxidant therapy reverses the impaired hematopoietic regeneration after 5-FU in H-Cx43-deficient mice and HSC/P Cx43 is required for ROS transfer to BM stromal cells. (*A* and *B*) In vivo NAC treatment restored PB recovery after 5-FU administration in H-Cx43-deficient mice. (*A*) Absolute neutrophil count (ANC). (*B*) Platelet count. ○, WT + PBS; ●, WT + NAC; □, H-Cx43-deficient + PBS; ■, H-Cx43-deficient + NAC. $*P < 0.05$, $n = 3$ mice per group. (*C* and *D*) ROS transfer from HSC/P cells into FBMD-1 stromal cells. Diagram of the coculture method (*Upper*). Green cells represent sorted LSK cells. Red areas represent nuclei containing the ROS reporter DHE. Orange arrows represent expected directional transfer of ROS. (*C–E*) Cx43 mediates ROS depletion from HSCs and uptake by BM stromal cells. (*C*) CFSE/DHE double-labeled HSC/P cells isolated from WT or H-Cx43-deficient mice were seeded onto FBMD-1 stromal cells for 3 h. Before coculture, sorted HSC/P cells were treated with LY83583 to induce ROS production, and FBMD-1 cells were treated with NAC for 16 h. Median fluorescent intensity of DHE in $CFSE^+$ HSC/P cells was measured by flow cytometry. (*D*) CFSE-labeled, sorted HSC/P cells from WT or H-Cx43-deficient mice were cultured with preformed DHE-labeled FBMD-1 stroma for 3 h. Before loading, HSC/P cells were treated with LY83583 to induce ROS and FBMD-1 cells had been treated with NAC for 16 h. MFI of DHE in FBMD-1 cells was measured by FACS. MFI of FBMD-1 cells preincubated or not with NAC was also analyzed. $*P < 0.05$, $**P < 0.01$. Data represent three independent experiments. (*E*) Sorted HSC/P cells from WT or H-Cx43-deficient mice were transduced with an empty vector or a Cx43-expressing lentiviral vector and cultured with preformed DHE-labeled FBMD-1 stroma for 3 h. Before loading, HSC/P cells were treated with LY83583 to induce ROS and FBMD-1 cells had been treated with NAC for 16 h. MFI of DHE in FBMD-1 cells was measured by FACS. $**P < 0.05$; $*P < 0.1$. Data represent two independent experiments. Empty bar, WT with empty vector transduction; black bar, H-Cx43-deficient with empty vector transduction; pink bar, WT with Cx43 transduction; red bar, H-Cx43-deficient with Cx43 transduction. Values represent means ± SD. (*F*) Neutrophil count of WT HM chimeric mice (open circles) and H-Cx43-deficient HM chimeric mice (solid circles) after 5-FU administration. $*P < 0.05$ ($n = 3$ mice per group). (*G* and *H*) BM cell and progenitor (CFU-C) content in two femurs, two tibia, and pelvis of WT HM (empty bars) and H-Cx43-deficient HM (solid bars) chimeric mice on day 11 postadministration of 5-FU. $*P < 0.05$ ($n = 3$ mice per group). Values represent means ± SD.

stromal cells. As a control, we checked that overnight NAC treatment of FBMD-1 cells significantly reduces the intracellular ROS levels (Fig. 4*D*). A 3-h coculture of WT HSC/P cells onto FBMD-1 reversed the effect of NAC, returning intracellular ROS levels similar to those in untreated FBMD-1 cells (Fig. 4*D*). However, H-Cx43-deficient HSC/P cells were unable to increase the transfer of ROS to FBMD-1 cells beyond the basal levels of NAC-treated FBMD-1 cells (Fig. 4*D*). Furthermore, exogenous expression of WT Cx43 in lentivirally transduced Cx43-deficient HSCs rescued the decreased transfer of ROS into the stromal cells in H-Cx43-deficient HSC/P cells to the same level of WT-Mock HSC/P cells (Fig. 4*E* and Fig. S6). Together, these data indicate that Cx43 mediates the transfer of ROS from HSC/P cells to hematopoiesis-supporting BM stromal cells.

Finally, to address whether Cx43 homotypic interactions between HSCs and BM stroma were at play, we analyzed whether Cx43 deficiency in the HM phenocopies the deficiency of Cx43 in the HSC compartment with respect to its inability to regenerate stress hematopoiesis. For this purpose, we induced Cx43 deficiency in the HM (10) using Mx1-Cre transgenic mice as shown previously (23, 32). Mx1-Cre;WT and Mx1-Cre;$Cx43^{flox/flox}$ mice were treated with polyinositide;polycytidine (polyI:C). One week after the last injection of polyI:C, the mice were submitted to lethal irradiation, followed by transplantation of WT CD45.1+ BM. Chimeric mice (>90% CD45.1+ hematopoietic chimera) were challenged with 5-FU in the same way as in primary Vav1-Cre;$Cx43^{flox/flox}$ mice. The myeloid regeneration of HM Cx43-deficient mice phenocopied the defective regeneration observed in H-Cx43-deficient mice, as assessed by neutrophil counts in the PB (Fig. 4*F*) and reduced BM cellularity and progenitor content (Fig. 4 *G* and *H*). This suggests that Cx43 expression in the HM is similarly required for hematopoietic regeneration and Cx43-Cx43 heterologous interactions between HSC/P cells and the cellular HM are required for an adequate regenerative response after chemotherapy.

Discussion

HSCs are responsible for sustaining blood formation and regeneration after injury for the entire lifespan of an organism through self-renewal, survival, proliferation, and differentiation. HSC aging has become a concern in chemotherapy of older patients. HSC function declines with age, and prolonged myelosuppression in response to cytotoxic chemotherapy drugs suggests a reduced marrow regenerative capacity in older individuals (33–36). However, the number of HSCs does not necessarily decline, but it can also increase (37, 38). There is evidence to indicate a distinct role for intrinsic and extrinsic factors in HSC aging to explain this apparent discrepancy (39). However, the molecular mechanisms that regulate the HM control on HSC function during aging are poorly understood.

HSC functions can be affected by the intracellular level of ROS that are produced endogenously through cellular metabolism or directly after exposure to exogenous stress, and ROS levels have long been associated with aging (40). At physiological levels, low and moderate levels of ROS appear to be required for HSC activity (41–43), including early hematopoietic reconstitution after transplantation (44). However, a sustained, abnormal increase in ROS production occurs under aging (24) and genotoxic stress (45), including 5-FU chemotherapy (46), which can inhibit HSC self-renewal and induce HSC senescence and hematopoietic dysfunction (24). Mimicking the situation in aged individuals, the HSC BM content of H-Cx43-deficient old mice is increased over aged-matched controls (47), whereas their ability to regenerate after 5-FU administration is diminished (Ref. 10 and Fig. 1 *J* and *K*). Followed by 5-FU administration, HSCs from H-Cx43-deficient mice showed decreased ability to enter the cell cycle and survive, as well as an increased intracellular ROS content.

In this report, we demonstrate a function of the HM as a scavenger of ROS from stressed HSC/P cells through Cx43. Our data provide evidence that Cx43 deficiency cannot be significantly compensated by other connexins, at either expression or functional levels, and Cx43 is a major mediator of ROS scavenging through transfer from HSCs to stromal cells.

It has been shown that ROS can regulate HSC function in a concentration-dependent manner. High levels of ROS can induce HSC senescence and apoptosis secondary to DNA damage (24). Whereas Cx43 deficiency induces increased apoptosis, surviving HSCs from H-Cx43-deficient mice display the hallmarks of senescence, including hyporegenerative capacity and cell cycle arrest after chemotherapy, and up-regulation of $p16^{INK4a}$. Hyporegenerative/senescent HSCs are induced by high levels of ROS/p38MAPK/Foxo1 signal activation, and HSC loss-of-function can be reverted by NAC administration in vivo or by the reintroduction of Cx43, indicating that Cx43 is a crucial molecule in the maintenance of HSC fitness. The reintroduction of Cx43 also rescues the ROS transfer from ROS^{high} HSC/P cells to BM stromal cells, confirming the expected role of HSC Cx43 in ROS scavenging by the HM. Finally, the deficiency of Cx43 in the HM in chimeric mice generated by transplanting WT hematopoiesis (>90%) into an inducible murine model of Cx43 deficiency (10) significantly phenocopies the deficiency of Cx43 in HSCs.

Altogether, our data provide insights into the homeostatic regulation of ROS content in BM HSCs and present a mechanism of BM microenvironment control on HSC activity through indispensable expression of Cx43 in both HSCs and the cellular HM.

Materials and Methods

Information on generation of H-/HM-Cx43-deficient and chimeric mice, repopulation experiments, drug administration and cell sorting, may be found in *SI Materials and Methods*. For HSC/P assays, including proliferation, cell cycle, survival and lentiviral transduction, see *SI Materials and Methods*. ROS transfer, genomic PCR, RT-PCR analysis, and statistical analysis are included in *SI Materials and Methods*.

ACKNOWLEDGMENTS. We thank Dr. Hartmut Geiger (University of Ulm) for helpful comments and Ms. Margaret O'Leary for editing the manuscript. We also thank Jorden Arnett, Jeff Bailey, and Victoria Summey for technical assistance and the Mouse and Research Flow Cytometry Core Facilities, both supported by National Institutes of Health/Centers of Excellence for Molecular Hematology Grant 1P30DK090971-01. This project was funded by the Heimlich Institute of Cincinnati (J.A.C.), US Department of Defense Grant 10580355 (to J.A.C.), National Institutes of Health Grants R01-HL087159 and HL08715951, the National Blood Foundation (D.G.-N.), Spanish Ministry of Science and Technology Consolider CSD2008-00005 (to L.C.B.), Community of Madrid Grant S2010/BMD-2460 (to D.G.-N.), and funds from the Hoxworth Blood Center and Cincinnati Children's Hospital Medical Center (to J.A.C.).

1. Kumar NM, Gilula NB (1996) The gap junction communication channel. *Cell* 84: 381–388.
2. Campbell FR (1980) Gap junctions between cells of bone marrow: An ultrastructural study using tannic acid. *Anat Rec* 196:101–107.
3. Yamazaki K (1988) Sl/Sld mice have an increased number of gap junctions in their bone marrow stromal cells. *Blood Cells* 13:421–435.
4. Dorshkind K, Green L, Godwin A, Fletcher WH (1993) Connexin-43-type gap junctions mediate communication between bone marrow stromal cells. *Blood* 82:38–45.
5. Krenacs T, Rosendaal M (1998) Connexin43 gap junctions in normal, regenerating, and cultured mouse bone marrow and in human leukemias: Their possible involvement in blood formation. *Am J Pathol* 152:993–1004.
6. Rosendaal M, Green CR, Rahman A, Morgan D (1994) Up-regulation of the connexin43+ gap junction network in haemopoietic tissue before the growth of stem cells. *J Cell Sci* 107:29–37.
7. Forsberg EC, et al. (2005) Differential expression of novel potential regulators in hematopoietic stem cells. *PLoS Genet* 1:e28.
8. Liu Y, et al. (2009) p53 regulates hematopoietic stem cell quiescence. *Cell Stem Cell* 4: 37–48.
9. Trowbridge JJ, Snow JW, Kim J, Orkin SH (2009) DNA methyltransferase 1 is essential for and uniquely regulates hematopoietic stem and progenitor cells. *Cell Stem Cell* 5: 442–449.
10. Presley CA, et al. (2005) Bone marrow connexin-43 expression is critical for hematopoietic regeneration after chemotherapy. *Cell Commun Adhes* 12:307–317.
11. Wilson A, et al. (2008) Hematopoietic stem cells reversibly switch from dormancy to self-renewal during homeostasis and repair. *Cell* 135:1118–1129.
12. Daria D, et al. (2008) The retinoblastoma tumor suppressor is a critical intrinsic regulator for hematopoietic stem and progenitor cells under stress. *Blood* 111: 1894–1902.
13. Ghiaur G, et al. (2008) Rac1 is essential for intraembryonic hematopoiesis and for the initial seeding of fetal liver with definitive hematopoietic progenitor cells. *Blood* 111: 3313–3321.
14. Wong PK, et al. (2006) SOCS-3 negatively regulates innate and adaptive immune mechanisms in acute IL-1-dependent inflammatory arthritis. *J Clin Invest* 116:1571–1581.
15. Sengupta A, et al. (2011) Atypical protein kinase C (aPKCzeta and aPKClambda) is dispensable for mammalian hematopoietic stem cell activity and blood formation. *Proc Natl Acad Sci USA* 108:9957–9962.
16. Essers MA, et al. (2009) IFNalpha activates dormant haematopoietic stem cells in vivo. *Nature* 458:904–908.
17. Cheng T, et al. (2000) Hematopoietic stem cell quiescence maintained by p21cip1/waf1. *Science* 287:1804–1808.
18. Bersenev A, Wu C, Balcerek J, Tong W (2008) Lnk controls mouse hematopoietic stem cell self-renewal and quiescence through direct interactions with JAK2. *J Clin Invest* 118:2832–2844.
19. Yilmaz OH, Kiel MJ, Morrison SJ (2006) SLAM family markers are conserved among hematopoietic stem cells from old and reconstituted mice and markedly increase their purity. *Blood* 107:924–930.
20. Chen J, et al. (2008) Enrichment of hematopoietic stem cells with SLAM and LSK markers for the detection of hematopoietic stem cell function in normal and Trp53 null mice. *Exp Hematol* 36:1236–1243.
21. Randall TD, Weissman IL (1997) Phenotypic and functional changes induced at the clonal level in hematopoietic stem cells after 5-fluorouracil treatment. *Blood* 89:3596–3606.
22. Janzen V, et al. (2006) Stem-cell ageing modified by the cyclin-dependent kinase inhibitor p16INK4a. *Nature* 443:421–426.
23. Walkley CR, Shea JM, Sims NA, Purton LE, Orkin SH (2007) Rb regulates interactions between hematopoietic stem cells and their bone marrow microenvironment. *Cell* 129:1081–1095.
24. Ito K, et al. (2006) Reactive oxygen species act through p38 MAPK to limit the lifespan of hematopoietic stem cells. *Nat Med* 12:446–451.
25. Balaban RS, Nemoto S, Finkel T (2005) Mitochondria, oxidants, and aging. *Cell* 120: 483–495.
26. Boengler K, et al. (2005) Connexin 43 in cardiomyocyte mitochondria and its increase by ischemic preconditioning. *Cardiovasc Res* 67:234–244.
27. Tothova Z, et al. (2007) FoxOs are critical mediators of hematopoietic stem cell resistance to physiologic oxidative stress. *Cell* 128:325–339.
28. Harris AL (2007) Connexin channel permeability to cytoplasmic molecules. *Prog Biophys Mol Biol* 94:120–143.
29. Schajnovitz A, et al. (2011) CXCL12 secretion by bone marrow stromal cells is dependent on cell contact and mediated by connexin-43 and connexin-45 gap junctions. *Nat Immunol* 12:391–398.
30. Ploemacher RE, Van der Loo JC, Van der Sluijs JP (1992) In vitro assays for primitive hematopoietic cells. *Blood* 79:834–837.
31. Knock GA, et al. (2009) Superoxide constricts rat pulmonary arteries via Rho-kinase-mediated Ca(2+) sensitization. *Free Radic Biol Med* 46:633–642.
32. Park D, et al. (2012) Endogenous bone marrow MSCs are dynamic, fate-restricted participants in bone maintenance and regeneration. *Cell Stem Cell* 10:259–272.
33. Appelbaum FR, et al. (2006) Age and acute myeloid leukemia. *Blood* 107:3481–3485.
34. Brunello A, et al. (2005) Adjuvant chemotherapy for elderly patients (≥70 years) with early high-risk breast cancer: A retrospective analysis of 260 patients. *Anal Oncol* 16: 1276–1282.
35. Morrison SJ, Wandycz AM, Akashi K, Globerson A, Weissman IL (1996) The aging of hematopoietic stem cells. *Nat Med* 2:1011–1016.
36. Sudo K, Ema H, Morita Y, Nakauchi H (2000) Age-associated characteristics of murine hematopoietic stem cells. *J Exp Med* 192:1273–1280.
37. de Haan G, Van Zant G (1999) Dynamic changes in mouse hematopoietic stem cell numbers during aging. *Blood* 93:3294–3301.
38. de Haan G, Nijhof W, Van Zant G (1997) Mouse strain-dependent changes in frequency and proliferation of hematopoietic stem cells during aging: Correlation between lifespan and cycling activity. *Blood* 89:1543–1550.
39. Woolthuis CM, de Haan G, Huls G (2011) Aging of hematopoietic stem cells: Intrinsic changes or micro-environmental effects? *Curr Opin Immunol* 23:512–517.
40. Harman D (1992) Role of free radicals in aging and disease. *Ann N Y Acad Sci* 673:126–141.
41. Juntilla MM, et al. (2010) AKT1 and AKT2 maintain hematopoietic stem cell function by regulating reactive oxygen species. *Blood* 115:4030–4038.
42. Kinder M, et al. (2010) Hematopoietic stem cell function requires 12/15-lipoxygenase-dependent fatty acid metabolism. *Blood* 115:5012–5022.
43. Owusu-Ansah E, Banerjee U (2009) Reactive oxygen species prime Drosophila haematopoietic progenitors for differentiation. *Nature* 461:537–541.
44. Lewandowski D, et al. (2010) In vivo cellular imaging pinpoints the role of reactive oxygen species in the early steps of adult hematopoietic reconstitution. *Blood* 115:443–452.
45. Wang Y, et al. (2010) Total body irradiation causes residual bone marrow injury by induction of persistent oxidative stress in murine hematopoietic stem cells. *Free Radic Biol Med* 48:348–356.
46. Hwang PM, et al. (2001) Ferredoxin reductase affects p53-dependent, 5-fluorouracil-induced apoptosis in colorectal cancer cells. *Nat Med* 7:1111–1117.
47. Flenniken AM, et al. (2005) A Gja1 missense mutation in a mouse model of oculodentodigital dysplasia. *Development* 132:4375–4386.